THE ASTROPHYSICAL JOURNAL, 492:205–212, 1998 January 1

A SURVEY OF HIGH-LATITUDE MOLECULAR GAS IN THE NORTHERN GALACTIC HEMISPHERE

DAP HARTMANN
Harvard-Smithsonian Center for Astrophysics, 60 Garden Street MS 72, Cambridge, MA 02138
LORIS MAGNANI
Department of Physics and Astronomy, University of Georgia, Athens, GA 30602
AND
PATRICK THADDEUS
Harvard-Smithsonian Center for Astrophysics, 60 Garden Street MS 72, Cambridge, MA 02138
Received 1997 March 6; accepted 1997 August 13

ABSTRACT

We surveyed the northern Galactic hemisphere (NGH) at $b \geq 30°$ in the CO (1–0) emission line to determine the surface filling factor of molecular gas at high Galactic latitudes and to search for heretofore unknown molecular clouds. The NGH was sampled on a locally Cartesian grid with 1° (true-angle) spacing in Galactic longitude and latitude. Of the 11,478 points in our grid, we observed all 10,562 positions that rise to an elevation above 30° in Cambridge, MA, the site of the 1.2 m millimeter-wave telescope that was used for the survey. Only 26 lines of sight showed CO emission. Monte Carlo simulations based on our sampling grid and with cloud sizes, in a uniform distribution, ranging from 0 to 2 deg^2 suggest that the survey is $\sim$70% complete. Power-law distributions yield fractional completenesses that are typically a factor of 2 lower. The surface filling factor, corrected for the incompleteness of our sampling grid, is 0.004–0.008, depending on which cloud size distribution is used. These values are substantially lower than what is found in the southern Galactic hemisphere at $b \leq -30°$. Adopting as the CO to H_2 conversion ratio $N_{H_2}/W_{CO} = 2.5 \times 10^{20}$ cm^{-2} (K km s^{-1})$^{-1}$, the mass surface density of molecular gas in the north ranges from 0.015 ± 0.009 to 0.035 ± 0.020 $M_\odot$ pc^{-2}. With the exception of four fairly significant aggregations of clouds (the complexes associated with the Polaris flare, Ursa Major, Draco, and L134), and a handful of isolated cloudlets, the northern Galactic hemisphere at $b \geq 30°$ is found to be largely free of molecular gas.

Subject headings: ISM: abundances — ISM: clouds — ISM: molecules — surveys

1. INTRODUCTION

The quantity of molecular gas at high Galactic latitudes ($b \geq 30°$) is not well known. Previous surveys have either been biased toward known objects (infrared cirrus, dark nebulae, or reflection nebulae), or were highly undersampled, or both. Consequently, key quantities such as the surface filling factor and the mass surface density of molecular gas at high latitudes are still largely unknown. Determining the distribution of high-latitude molecular clouds has implications beyond ascertaining the completeness of the local molecular gas inventory. A complete catalog of high-latitude clouds might lead to a better understanding of the local bubble of hot gas and X-ray shadowing as well (e.g., Snowden, McCammon, & Verter 1993). Moreover, some high-latitude clouds are forming stars; any inventory of local star formation must take into account these objects given their proximity to the Sun (Magnani et al. 1995).

High-latitude molecular gas as a rule is tenuous and fairly translucent (van Dishoeck et al. 1991) and has lower densities and higher $^{12}CO/^{13}CO$ line ratios than dark clouds or giant molecular clouds (GMCs; Polk et al. 1988). Recent studies of the $^{12}CO/^{13}CO$ ratio in several regions near the Galactic plane (Polk et al. 1988) and of the CO (2–1)/CO (1–0) line ratio in the Milky Way molecular ring (Chiar et al. 1994) imply that up to 58% of the molecular cloud ensemble may be composed of translucent gas. Because the outer regions of GMCs are composed of gas with relatively low density and opacity compared with that in the dense star-forming interior (e.g., Heyer, Carpenter, & Ladd 1996), a substantial portion of even large clouds may be fairly translucent in nature. Thus, the translucent emission noted by Polk et al. (1988) in the Galactic plane could arise primarily from these regions rather than from an ensemble of isolated translucent clouds.

To understand these observations better and to assess the importance of translucent clouds in the molecular mass inventory of the interstellar medium (ISM), we conducted a survey of high-latitude molecular clouds in the northern Galactic hemisphere (NGH).

Several large complexes of high-latitude molecular clouds have been identified and studied in the NGH. One of these, the Ursa Major cloud complex, is the largest aggregation of translucent gas at $b \geq 30°$, covering at least 13 deg^2 and containing 50–220 $M_\odot$ of molecular gas, depending on the distance estimate (Heithausen et al. 1993; Magnani, Hartmann, & Speck 1996, hereafter MHS). Small portions of this cloud complex were first identified by Magnani, Blitz, & Mundy (1985, hereafter MBM), and a complete map of the region was made by de Vries, Heithausen, & Thaddeus (1987). These molecular clouds are located close to the Polaris flare, a large molecular cloud ($M \sim 2000$ $M_\odot$) situated at $117° \leq l \leq 128°$ and $20° \leq b \leq 32°$, discovered by Heithausen & Thaddeus (1990). It is not clear whether the Ursa Major cloud complex and the Polaris flare are physically related. Infrared emission and 21 cm H I maps show a large contiguous arc or loop of gas and dust encompassing both objects (Meyerdierks, Heithausen, & Reif 1991) but distance estimates vary considerably, from 100–120 pc for

clouds in the Ursa Major complex (Penprase 1993) to 240 pc for the Polaris flare (Heithausen et al. 1993).

Other well-studied high-latitude molecular complexes in the NGH are the Draco clouds, first identified by Goerigk et al. (1983); the north celestial pole clouds described by Heithausen et al. (1993); and the clouds associated with the dark cloud L134, north of the ρ Ophiuchi complex (Clark & Johnson 1981; MHS). Several other isolated clouds at $b \geq 30°$ were identified by MBM and by Heiles, Reach, & Koo (1988). The only systematic survey prior to the present one was that of a 620 deg^2 region between $117° \leq l \leq 160°$ and $16° \leq b \leq 42°$ (Heithausen et al. 1993). The surface filling factor of the CO (1–0) transition from that study (defined as ϵ_b, where b is the Galactic latitude) was much higher ($\epsilon_{16-42} = 0.13$) than found from an earlier survey by Magnani, Lada, & Blitz (1986), who sampled the high-latitude sky in random directions and determined that $\epsilon_{|25-90|} \sim 0.005$. Estimates for the mass surface density of molecular gas at $|b| \geq 25°$, $\Sigma_{|b|\geq 25}$, currently range from 0.2 $M_\odot$ pc^{-2} (Magnani et al. 1986; MHS) to 0.9 $M_\odot$ pc^{-2} (Heithausen et al. 1993).

In an attempt to resolve the issue and to identify any large, undiscovered molecular cloud complexes, we have surveyed the entire NGH at $b \geq 30°$ for those directions that transit at an elevation greater than 30° in Cambridge, MA (latitude $+42°22'$). The survey, which samples the NGH every degree in Galactic longitude and latitude, is complete for all $\delta \geq -17\overset{\circ}{.}6$ (i.e., 92% of the region $b \geq 30°$). The specifics of the grid pattern are discussed in § 2. Because some high-latitude clouds are smaller than our grid spacing, a number may have gone undetected. To address this problem, Monte Carlo simulations (described in the Appendix) were used to estimate the completeness of the survey.

The small scale height of the ISM at the solar circle suggests that most of the clouds at $b \geq 30°$ are nearby (MHS). The results of the present survey (presented in § 3 and summarized in § 4), when combined with H I and infrared data, provide a fairly complete inventory of the high-density ($n > 10^2$ cm^{-3}) gas content of the local northern hemisphere ISM.

2. SURVEY METHODOLOGY AND OBSERVATIONAL SETUP

2.1. *The Search Grid*

The average surface area of high-latitude molecular clouds is approximately 1 deg^2 (MHS). To ensure detecting nearly all clouds of this size, we sampled the NGH on a locally Cartesian grid with 1° (true-angle) spacing in l and b. For ease of carrying out the observations we used equally spaced intervals in longitude (Δl) for 6° wide latitude strips. We chose Δl to be the nearest truncated multiple of $0\overset{\circ}{.}1$ equal to $1\overset{\circ}{.}0/\cos b_{\rm min}$, where $b_{\rm min}$ is the latitude closest to the Galactic plane for the latitude strip. Thus, the true-angle sampling interval, $\Delta l \times \cos b$, was always $\leq 1\overset{\circ}{.}0$, generally in the range $0\overset{\circ}{.}8$–$1\overset{\circ}{.}0$. Table 1 lists the various Δl intervals that were used at a given latitude and the corresponding effective (true-angle) sampling intervals, $\Delta l \times \cos b$. The

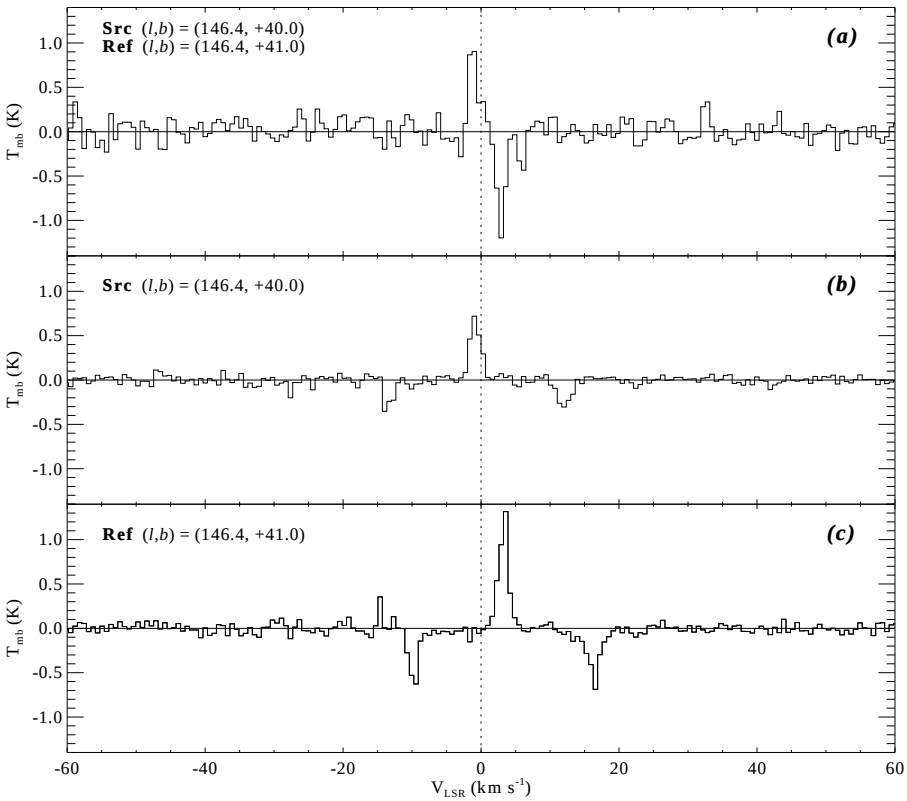

FIG. 1.—(*a*) Position-switched CO (1–0) spectrum of MBM 31 from the NGH survey. The high-latitude cloud is detected in both the "source" and the "reference" spectrum. The presence of CO emission in the reference spectrum results in an "absorption" line to the right of the emission line from the source spectrum. The velocity resolution of the data is 0.65 km s^{-1} and the rms noise level is 0.1 K. A third-order baseline was removed from the spectrum. (*b*, *c*) Frequency-switched spectra of the individual source (*b*) and reference (*c*) positions that were detected in (*a*). The difference in central velocity and intensity of these two lines guaranteed the original detection. The rms noise level is ≤ 0.05 K, and the parameters listed in Table 2 were derived from Gaussian fits made to the line profiles.

TABLE 1

SAMPLING INTERVALS

$\|b\|$ (deg)	Δl (deg)	Sampling Interval[a] (deg)
30, 32, 34.....	1.1	0.95, 0.93, 0.91
36, 38, 40.....	1.2	0.97, 0.95, 0.92
42, 44, 46.....	1.3	0.97, 0.94, 0.90
48, 50, 52.....	1.5	1.00, 0.96, 0.92
54, 56, 58.....	1.7	1.00, 0.95, 0.90
60, 62, 64.....	2.0	1.00, 0.94, 0.88
66, 68, 70.....	2.4	0.98, 0.90, 0.82
72, 74, 76.....	3.2	0.99, 0.88, 0.77
78, 80, 82.....	4.8	1.00, 0.83, 0.67
84, 86, 88.....	9.5	0.99, 0.67, 0.33

[a] The sampling interval is $\Delta l \times \cos b$.

sampling grid has 11,478 points, but 8% of the NGH at $b \geq 30°$ never rises above our elevation limit of 30°. Therefore, the actual number of grid points observed in the NGH is slightly less: 10,562.

2.2. *Telescope and Observing Configuration*

A standard tracer for molecular gas, and generally the easiest one to observe, is the CO (1–0) transition at 115 GHz. There are apparently a few locations where the CH ground-state hyperfine main line transition at 3.3 GHz and the equivalent OH transitions at 1.6 GHz trace molecular gas that is undetectable in CO (e.g., Wannier et al. 1993; Magnani et al. 1997), but the integration times required to detect weak OH or CH emission are generally much too long for survey work. Consequently, the CO (1–0) line was used exclusively here to search for high-latitude molecular gas.

The 1.2 m millimeter-wave telescope of the Harvard-Smithsonian Center for Astrophysics is the most suitable instrument for CO survey work on this scale. This instrument (described in detail by Cohen, Dame, & Thaddeus 1986) has an 8′.4 main-beam size (FWHM) at 115 GHz, and the main-beam efficiency is 0.82 (Dame 1995). The pointing accuracy is better than 1′, or 12% of the size of the main beam. The SIS receiver (see Dame et al. 1993 for a description) has a single-sideband noise temperature of less than 70 K. For low atmospheric opacity and high elevation, the total system temperature is typically less than 400 K. The back end consists of two 256 channel filter banks with channel spacings of 0.50 MHz (1.30 km s^{-1}) and 0.25 MHz (0.65 km s^{-1}). The high-resolution filter bank samples the central 128 channels of the low-resolution filter bank. By matching their total powers in the region of overlap, a check is provided that enables identification and subsequent correction of bad channels in the velocity range $v_c - 83 \leq v_c \leq v_c + 83$ km s^{-1}, where v_c is the LSR velocity on which the back end is centered ($v_c = 0$ km s^{-1} for the entire survey). The outermost 64 channels on either side of the low-resolution filter bank are appended to the high-resolution spectrum to yield a 384 channel spectrum that spans a velocity range of 333 km s^{-1}.

2.3. *Position-Switching Technique*

In the first stage of the project, we were mainly concerned with detecting new high-latitude clouds, not determining their structure in detail. Because of the ubiquitous presence of terrestrial CO line emission from the upper atmosphere

TABLE 2

CO $J = 1$–0 DETECTIONS

Detection	l (deg)	b (deg)	T_{mb}[a] (K)	v_{LSR} (km s^{-1})	Δv (km s^{-1})	$\Sigma T\, dv$ (K km s^{-1})	Identification[b]
1	123.2	30.0	0.31 ± 0.05	0.1	1.2	0.93 ± 0.19	Polaris flare
2	124.3	30.0	1.30 ± 0.05	0.9	0.8	2.57 ± 0.29	Polaris flare
3	123.2	31.0	0.17 ± 0.05	−0.8	0.9	0.36 ± 0.22	Polaris flare
4	124.3	31.0	0.27 ± 0.02	−0.7	0.8	0.53 ± 0.09	Polaris flare
5	141.9	35.0	1.00 ± 0.05	−0.6	0.6	1.42 ± 0.19	MBM 27
6	4.8	36.0	0.78 ± 0.05	1.3	0.7	1.44 ± 0.27	MBM 34
7	6.0	36.0	0.50 ± 0.05	1.9	1.1	1.33 ± 0.28	L134N, L169, L183–4
8	153.6	36.0	3.42 ± 0.05	−2.4	0.7	6.33 ± 0.20	HSVMT 27
9	4.8	37.0	5.18 ± 0.05	3.4	0.9	11.30 ± 0.22	MBM 34
10	6.0	37.0	1.48 ± 0.05	2.2	0.9	3.35 ± 0.21	L134N, L169, L183–4
11	10.8	37.0	0.65 ± 0.04	1.5	0.5	0.82 ± 0.18	MBM 39, S36
12	91.2	37.0	0.98 ± 0.04	−24.9	1.2	2.91 ± 0.19	Draco
13	147.6	37.0	0.85 ± 0.05	−2.0	0.7	1.46 ± 0.19	HSVMT 24
14	153.6	37.0	2.14 ± 0.05	−1.1	0.9	5.07 ± 0.20	HSVMT 27
15	91.2	38.0	0.30 ± 0.03	−22.3	0.8	0.59 ± 0.12	Draco
16	142.8	38.0	0.51 ± 0.05	1.9	0.6	0.80 ± 0.21	MBM 30
17	148.8	38.0	1.36 ± 0.05	−0.2	0.7	2.24 ± 0.21	HSVMT 24
18	14.4	39.0	0.15 ± 0.03	1.2	0.5	0.18 ± 0.08	New detection
19	90.0	39.0	0.88 ± 0.03	−23.9	1.6	3.43 ± 0.13	Draco
20	148.8	39.0	0.09 ± 0.02	−3.1	0.9	0.21 ± 0.08	HSVMT 24
21	150.0	39.0	0.44 ± 0.05	0.1	0.8	0.86 ± 0.18	HSVMT 27
22	146.4	40.0	0.69 ± 0.04	−0.9	0.8	1.45 ± 0.18	MBM 31
23	147.6	40.0	0.51 ± 0.05	−0.2	1.1	1.35 ± 0.19	MBM 32
24	146.4	41.0	1.17 ± 0.05	3.3	0.8	2.24 ± 0.20	MBM 31
25	136.5	43.0	0.29 ± 0.05	8.5	0.7	0.50 ± 0.18	New detection
26	37.7	45.0	0.31 ± 0.09	3.1	0.7	0.51 ± 0.34	MBM 40

[a] Antenna temperature (T_A^*) corrected for the main-beam efficiency of the telescope.

[b] This column lists the principal cloud or complex identified with the detection. Other nearby clouds may also be associated with the detected position. See MHS for a complete list of all previously known high-latitude clouds.

at roughly 80 km (Allen, Yung, & Waters 1981), frequency switching (FS) is not a good choice for a survey like the present one. Unless the telluric line can be accurately modeled and subtracted, there is always the possibility that it will mask part of the astronomical emission. Only when the velocity extent of the emission is known can FS be used to observe interstellar CO.

The previous surveys of the NGH (Magnani et al. 1986; Heithausen et al. 1993) did not detect many new molecular clouds. Consequently, the current search for high-latitude molecular clouds was undertaken by position switching (PS). If a tentative detection was made, it was followed by a series of FS observations, with care taken that the velocity of the telluric line was not coincident with the velocity of the suspected astronomical line. Additionally, we modeled the atmospheric line from the same data set of FS spectra, and subtracted the model to obtain "clean" FS spectra.

In position switching, the spectrum at a nearby reference position is subtracted from that at the position under observation, in order to remove the atmospheric line as well as baseline irregularities of instrumental origin. To avoid the laborious and error-prone procedure of establishing a large net of emission-free reference positions, we adopted a method that dispenses with this requirement entirely. Two targeted directions were obtained during the course of one scan by taking the source position at an even-numbered Galactic latitude and switching it against a reference position at a latitude 1° to the north.

Position switching of this kind has one potential drawback: equal amounts of emission from the source and reference directions will cancel out, and even strong signals may disappear. The chances of this happening are small, however, because the following conditions must hold: (1) the cloud must extend over at least 1°; (2) the emission must occur at precisely the same velocity and must have the same velocity dispersion for both directions; (3) the intensity must be equal in both directions. It is unlikely for all three conditions to be true simultaneously, except for large uniform objects that will always be detected at their edges. This issue along with other completeness considerations will be discussed in § 3.2.

3. RESULTS

3.1. *Observations and Data Reduction*

The present survey was carried out from 1995 March to May and from 1995 October to 1996 May. The 10,562 grid points (as described in § 2.1) were measured using PS with 5281 pairs of source and reference grid points. The telescope control program is set up such that a target rms noise level (σ) for the spectrum, from which the actual integration time will be calculated, is specified. Because the sensitivity of the receiver depends on the atmospheric opacity, and so varies with elevation and time, a better, more uniform survey is achieved by specifying the rms noise level, not the integration time. We chose $\sigma = 0.1$ K (T_A^*), which requires integration times of 2–15 minutes, with a mean of about 5 minutes.

Bad channels in the high-resolution filter bank were corrected (see § 2.2), and a third-order polynomial baseline was subtracted using the automated iterative method described by Hartmann (1994).

Every spectrum was visually inspected for the presence of emission lines. A simple computer algorithm was also used to flag the presence of a potential line. Figure 1 shows our "double detection" of MBM 31 observed in PS mode (*a*) and the FS line profiles of the individual "source" (*b*) and "reference" (*c*) positions.

3.2. *Detections*

All tentative detections were reobserved in PS with higher sensitivity ($\sigma \leq 0.05$ K). If a detection was confirmed, both the source and the reference positions were observed by FS to obtain the physical parameters of the line. The rms noise for these spectra was ≤ 0.05 K in T_A^*, corresponding to ≤ 0.06 K in $T_{\rm mb}$ (see Dame 1995).

Emission exceeding a 3 σ main-beam brightness temperature level ($T_{\rm mb} \geq 0.18$ K) was detected from 26 positions, 24 of which coincided with previously known molecular clouds. In Table 2 we list the Galactic coordinates of the detections, along with the Gaussian fit parameters to the emission lines, and any previous identifications. Figure 2 shows the distribution of the detected clouds (*black circles*) on our sampling grid (*grid points*). The gray diamonds identify the positions of the NGH high-latitude clouds (from MHS) that were not detected in our survey.

Only two new clouds were discovered. The 6 σ detection at (l, b) = (136°.5, +43°.0) is only a few degrees away from the Ursa Major cloud complex, and may be related to it. The 5 σ detection at (l, b) = (14°.4, +39°.0) may be part of the string of clouds associated with L134, north of the ρ Ophiuchi region. Of the 26 positions we detected, 11 (12, if we include one of the new detections) are part of the Ursa Major cloud complex, four belong to the Polaris flare, three are part of the intermediate-velocity Draco cloud complex, and five (six, if we include the other new detection) are part of the L134 complex. Only one detection is associated with an isolated cloud (MBM 40), which covers an area of ~ 0.5 deg^2.

Because more than 26 clouds are known to exist in the NGH (MHS), some objects may have been missed because the sampling grid was too coarse. Although we discuss this topic in detail in the Appendix, we can make a preliminary estimate. There are 20 objects at $b \geq 30°$ listed in the MBM compilation of high-latitude molecular clouds. Most of the 24 previously known detections are associated with 12 of the northern clouds listed by MBM. The remaining eight MBM clouds were not detected in our survey because of the undersampling (i.e., falling through the sampling grid). Figure 3 shows as an example (*a*) how MBM 25 was missed and (*b*) how MBM 30 was nearly missed by our sampling grid. A rough estimate of the completeness is thus 60%, which agrees with the fractional completeness as determined from Monte Carlo simulations (see the Appendix).

We note that none of the isolated cirrus clouds reported by Heiles et al. (1988) and Reach, Koo, & Heiles (1994) were detected (with the exception of two lines of sight in the Draco cloud complex), almost certainly because of their small sizes. They are, in general, mostly atomic, isolated, degree-sized condensations selected on the basis of their H I and infrared emission properties—a technique very different from that used by MBM or Keto & Myers (1986). Approximately half of the isolated cirrus clouds have CO emission in core regions that are substantially smaller than 1 deg^2, and so are more likely to be missed in our survey than the larger MBM clouds. In the Appendix we estimate what fraction of the clouds we expect to have missed, given our sampling grid and sensitivity for various cloud size distributions.

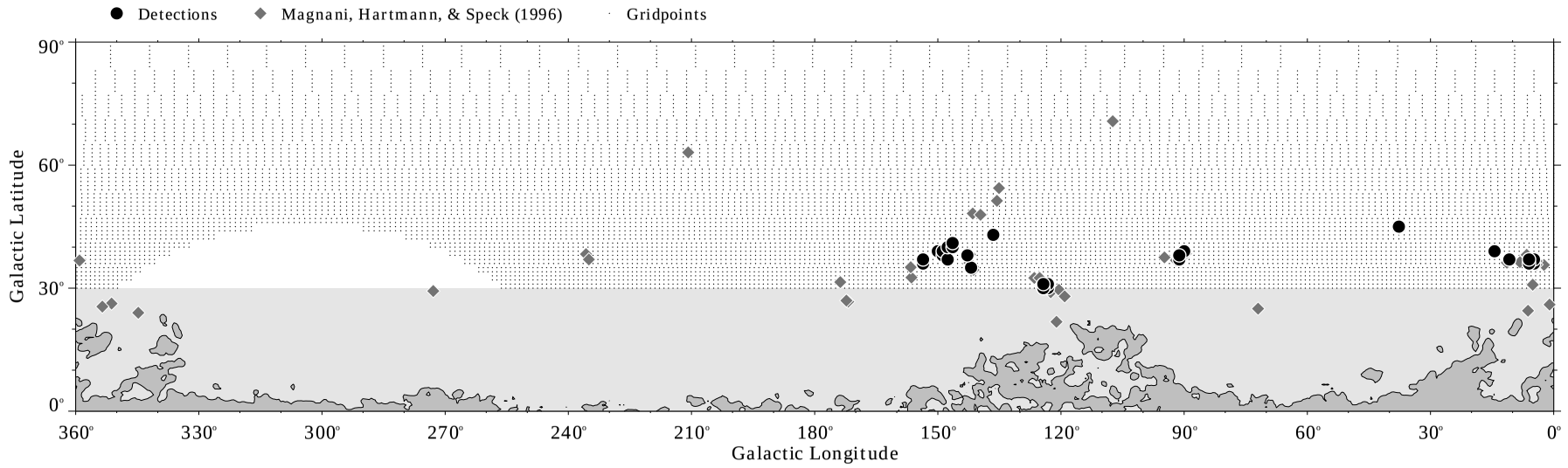

FIG. 2.—Distribution of high-latitude clouds and grid points surveyed during the course of the NGH survey. Black circles are the detections found in the survey, and gray diamonds identify known molecular clouds that were missed by our sampling grid (*grid points*). The filled contours are the Dame et al. (1987) superbeam CO survey at the $\Sigma T_{\rm mb}\, dv = 2$ K km s^{-1} level.

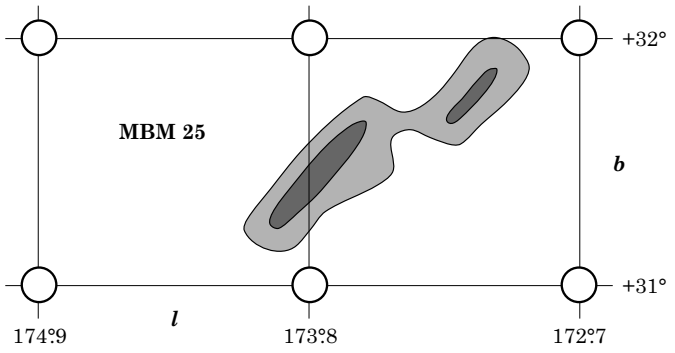

FIG. 3a

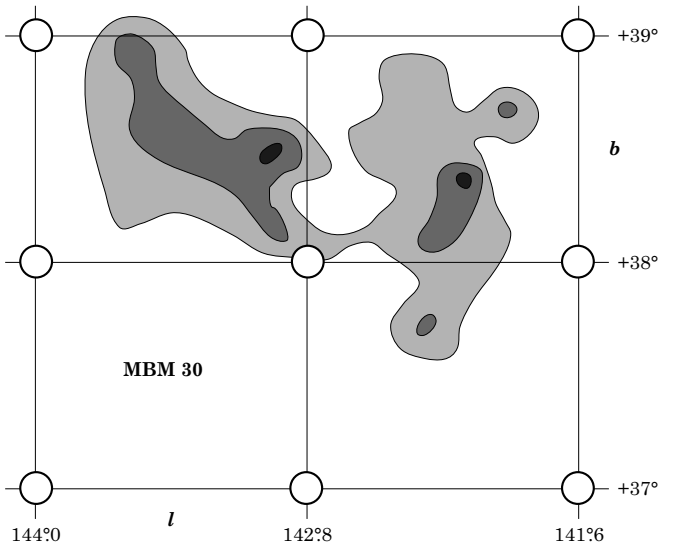

FIG. 3b

FIG. 3.—(*a*) CO (1–0) map (adapted from MBM) of the high-latitude cloud MBM 25 shows how our sampling grid pattern missed this object. The lowest contour is at 0.5 K (peak temperature), so it is unlikely that any significant molecular gas extends much beyond this contour. The circles represent the beam of the 1.2 m Harvard-Smithsonian millimeter-wave telescope (FWHM = 8′.4). (*b*) CO (1–0) map (adapted from MBM) of the high-latitude cloud MBM 30. This object managed to defy our sampling grid, except at $(l, b) = (142°.8, +38°.0)$, which was switched against the "reference" at $b = +39°.0$. It is detected at the lowest (0.5 K) contour level (peak temperature) in this map, which corresponds to the 5 σ level for our survey (see Table 2).

3.3. *The Surface Filling Factor and the Mass Surface Density in the NGH*

The surface filling factor for the NGH at $b \geq 30°$, $\epsilon_{\geq 30}$, can be expressed as the number of detections divided by the number of points in the survey. We find that $\epsilon_{\geq 30} \sim 0.0025/\eta$, where η is the fractional completeness of the survey based on sampling and sensitivity considerations ($\eta = 0.3$–0.7; see the Appendix). The 916 points that were not observed owing to the elevation limit are unlikely to change our conclusion that the NGH is largely devoid of molecular gas. In contrast, the southern Galactic hemisphere (SGH) is significantly richer in molecular clouds (see MHS). A survey of the SGH is currently in progress using the CfA 1.2 m telescope, and 2 dozen new molecular clouds have already been found.

MHS showed that the north-south asymmetry in the distribution of local molecular clouds can be explained as a displacement of the Sun from the Galactic midplane, but it may also be a consequence of the structure of the local bubble. If the Sun is displaced above the Galactic midplane and the local bubble is actually a "chimney" or "worm" of the kind described by Norman (1990) and Heiles (1990, 1992), then hot gas in the bubble can vent into the Galactic halo in the direction of the north Galactic pole (NGP). A small molecular cloud in the path of this hot buoyant gas quite possibly would not survive the encounter (Cowie & McKee 1977). An alternative explanation for the absence of clouds at $b > 70°$ is that the neutral gas has been swept up far enough from the plane so that the density and pressure of the ambient ISM at the new location may prevent the formation of molecular gas (e.g., Elmegreen 1993).

Liszt (1994) came to essentially the same conclusion about the paucity of clouds in the NGH, in a survey of local CO absorption toward extragalactic millimeter-wave continuum sources. We stress that our survey indicates only the absence of *molecular* gas in the direction of the NGP. Several studies show that significant extinction exists in this direction, probably at the northern boundaries of the local bubble (e.g., Hilditch, Hill, & Barnes 1976; Knude 1979; Kilkenny 1980; Perry & Johnston 1982).

With the value of $\epsilon_{\geq 30}$ determined above, the mass surface density $\Sigma_{\geq 30}$ can be estimated. The volume of the region encompassing the detections must first be determined. The data presented by MHS permit the calculation of the average distance of a high-latitude cloud projected onto the Galactic midplane. Using the average cos b for the 120 clouds tabulated by MHS (0.780 ± 0.137), and assuming a mean distance to the high-latitude clouds of 260 pc (determined from the velocity dispersions of the ensemble; see MHS), the projected distance onto the plane is 200 ± 35 pc. Using this value as the radius of a cylindrical volume centered on the Sun, the surface area of the top of the cylinder looking down onto the Galactic plane is $(1.26 \pm 0.31) \times 10^5$ pc^2. We will use this value as the surface area within which are projected the high-latitude clouds in our sample when viewed from above (or below) the Galactic plane.

MHS compiled masses from the literature for about 50 of the 120 high-latitude clouds. Although the mass determinations are based on different techniques and differing values of the CO to H_2 conversion factor, X_{CO}, the average cloud mass is 41 $M_\odot$. The uncertainty in this value arises from the uncertainty in the W(CO) observations and from the uncertainty in X_{CO}. In most typical molecular cloud mass determinations the mass is the product of the two aforementioned quantities. The uncertainty in W(CO) is typically 10%. The value of X_{CO} can vary by an order of magnitude over the ensemble of translucent clouds (Magnani et al. 1997). However, for a given cloud, X_{CO} can be determined to about 50% (Magnani et al. 1997). Following MBM, we used $X_{CO} = 2.5 \times 10^{20}$ cm^{-2} (K km s^{-1})$^{-1}$. Assuming that the clouds detected during the course of our survey have a mean mass of 41 ± 21 $M_\odot$, and accounting for the incompleteness of our survey, the total molecular

mass of the $26\eta = 37$ clouds is $1520 \pm 770\ M_\odot$. Correcting for the helium content of the clouds leads to an estimated total mass for the molecular clouds in the NGH of $1920 \pm 970\ M_\odot$. With these estimates, $\Sigma_{\geq 30} = 0.015 \pm 0.009\ M_\odot\ \mathrm{pc}^{-2}$ for $\eta = 0.7$ and $0.035 \pm 0.020\ M_\odot\ \mathrm{pc}^{-2}$ for $\eta = 0.3$.

These values are substantially lower than the local mass surface density of high-latitude clouds derived by MHS, 0.2–0.3 $M_\odot\ \mathrm{pc}^{-2}$ (which included the southern hemisphere contribution). Moreover, compared with the Σ of local molecular clouds at lower latitudes (0.5–2.0 $M_\odot\ \mathrm{pc}^{-2}$; MHS), the contribution of high-latitude molecular gas in the NGH to the total local molecular mass is negligible.

4. SUMMARY

We have surveyed the northern Galactic hemisphere at latitudes $b \geq 30°$, a total area of 10,315 deg^2 in the CO (1–0) transition. With our 8.′4 beam we have undersampled this region by about a factor of 50. However, given the size distribution of the previously known molecular clouds, our method of wide-meshed surveying is believed to be complete to within 30%–70%, depending on which model for the cloud size distribution is chosen. We have detected only two new molecular clouds, which may be part of the extended Ursa Major region and the L134 complex. The value of the surface filling factor for the NGH is found to be $\epsilon_{\geq 30} \sim 0.004$–$0.008$ and the mass surface density $\Sigma_{\geq 30} \sim (0.015 \pm 0.009)$–$(0.035 \pm 0.020)\ M_\odot\ \mathrm{pc}^{-2}$. There is much less molecular gas in the northern Galactic hemisphere than in the southern Galactic hemisphere. With the exception of four major cloud complexes (Polaris flare, Ursa Major, Draco, and L134), the NGH at high Galactic latitudes contains very little molecular gas.

L. M. acknowledges partial support from NASA grant NAG 5-2665. We wish to thank Tamerleigh Grenfell and Amy Philbrick for carrying out part of the observing. We acknowledge helpful suggestions from an anonymous referee, particularly in regard to the discussion of the completeness of the survey.

APPENDIX

EXPECTED COMPLETENESS OF THE SURVEY

Although over 10,000 lines of sight were observed, the 8.′4 beam has considerably undersampled the NGH (by about a factor of 50), so the issue of completeness of the survey must be addressed. Even with a telescope such as the CfA 1.2 m, which has been devoted to this project for 25% of the last two observing seasons, time is limited. For this survey to be meaningful, it had to exceed the sensitivity of the MBM survey to guarantee the detection of at least those clouds, should the observing grid intersect them (see Fig. 3). With this constraint, a grid sampling of 1° was the best attainable given the time restrictions (the goal was to complete both the NGH and the SGH visible from Cambridge, MA, in three observing seasons). As the average size of most high-latitude clouds is of the order of 1 deg^2 (MHS), a few would certainly be missed. On the other hand, increasing the grid sampling to, say, 0.°5 would decrease the sensitivity by a factor of 2. We believe that the present observing parameters strike about the best balance.

With the sampling grid as described in § 2.1, it is fair to assume that virtually all clouds larger than 1 deg^2 have been detected. Of course, an extended filamentary cloud might "snake" its way around our grid points and thus conspire to remain undetected (MBM 30 comes close to doing that; see Fig. 3). However, the real problem is to determine how many objects smaller than 1 deg^2 we have missed.

To answer this question, a Monte Carlo simulation was run in which, as a first attempt to parameterize the distribution of cloud sizes, a uniform random distribution of clouds was generated, ranging in size from 0 to 2 deg^2 (actually, the minimum size allowed was 0.02 deg^2). The filling factor for molecular clouds in the NGH was assumed to be 0.01. For the high-latitude sky at $b \geq 30°$, this value implies that ~ 103 deg^2 are covered with molecular gas. The Monte Carlo simulation randomly assigned solid angles from the specified range to the clouds, until the sum of the cloud areas reached the total surface area. For a cloud sample with a solid-angle upper limit of 2 deg^2, this coverage is achieved typically with 94–114 clouds. These objects were then placed randomly in the NGH at $b \geq 30°$. Next, the program determined how many grid points there were within a distance less than or equal to the difference between the cloud radius and the beam radius.

Two dozen simulation runs indicated that with a uniform distribution of cloud sizes in the 0–2 deg^2 range, our sampling pattern would detect 0.67 ± 0.07 of all the clouds in the NGH. Decreasing the maximum cloud size to 1 deg^2 lowered the fraction of clouds detected to 0.37 ± 0.04. For maximum cloud sizes of 0.75 deg^2 the fraction detected drops to the 0.2–0.3 range, while maximum cloud sizes of 0.5 deg^2 result in the detection of only ~ 0.2 of all the clouds.

If the fractional completeness η is expressed as the product of a sampling component η_{samp} and a sensitivity component η_{sens}, then the simulations indicate that for cloud sizes similar to those found by MHS, $\eta_{\mathrm{samp}} \sim 0.7$. The sensitivity component η_{sens} is not expected to differ much from unity. By integrating down to antenna temperatures of 0.1 K rms, CO column densities of order 10^{15} cm^{-2} are detectable, guaranteeing the detection of any translucent-type cloud, provided it is not substantially smaller in angular extent than the telescope beam size. Clouds with $N(\mathrm{CO}) < 10^{15}$ cm^{-2} are traditionally known as "diffuse molecular clouds" and are studied almost exclusively using high-resolution optical and UV spectroscopy. We therefore assume that η_{sens} is unity, $\eta_{\mathrm{samp}} = 0.7$, and, thus, $\eta = 0.7$.

Although the above analysis seems reasonable, it has long been established that the sizes of interstellar clouds in the Galaxy follow a power-law distribution rather than a uniform distribution (Dickey & Garwood 1989; Scalo 1985). Unfortunately, this more realistic situation is difficult to model because determinations of the cloud size distributions are beset by problems ranging from sampling and sensitivity considerations to uniformly defining the boundary of a cloud (Scalo 1985). In addition, a turnover, or cutoff in the power-law distribution of the number of molecular clouds as a function of linear size or area, has never been established successfully (Dickey & Garwood 1989).

We assumed that the clouds are spherical and imposed a cutoff in the cloud size distribution of 0.°1 in radius (corresponding to an area for a circular cloud of 0.03 deg^2). At a distance typical of high-latitude clouds (100 pc; MHS), 0.°1 corresponds to a cloud of less than 0.2 pc in radius, a value near the lower size limit for observed molecular entities (Elmegreen 1993). In addition, any cloud much smaller than 6′ in radius would be beam diluted by the 8.′4 angular resolution of our telescope, and thus be less likely to be detected.

With these caveats in mind, we ran a Monte Carlo simulation for a series of power-law distributions where the number of clouds as a function of radius is of the form

$$N(r) = N_0\left(\frac{r}{r_0}\right)^{-\alpha}$$

where N_0 and r_0 are normalization constants and α is an exponent that ranges from 1.0 to 1.3 (Scalo 1985). The power-law distributions perforce have more small clouds than the uniform distribution, so that the number and proportion of small clouds in the simulation will increase, decreasing the completeness factor. For power laws with α indices of 1.0, 1.2, and 1.3, the fractional completeness η was found to be 0.42 ± 0.03, 0.33 ± 0.02, and 0.28 ± 0.03, respectively. Thus, for standard cloud size spectra, $\eta_{\rm samp}$ is in the 0.3–0.4 range.

Finally, we simulated the completeness of the actual cloud size distribution from MHS. For convenience, all clouds larger than 1° were treated as exactly 2° in linear size (there were 17 of this type), and all clouds smaller than 0.°4 in linear size (20) were treated as exactly 0.°2 in extent. From these "diameters," surface areas were obtained based on the assumption of spherical clouds. A total of 78 clouds were included in the sample, and the resulting value for $\eta_{\rm samp}$ after 20 Monte Carlo runs was 0.56 ± 0.08.

In summary, a more realistic size distribution for clouds leads to values of $\eta_{\rm samp}$ in the 0.3–0.6 range. The uncertainty introduced when the power-law index of cloud sizes is not known is of the same order as the uncertainty in $\eta_{\rm samp}$ estimated in § 3.2. We note that mapping all the detections in this survey would lead to an unbiased estimate of the power-law index for clouds in the NGH. Until such a project is carried out, we will have a factor of 2 uncertainty in η.

REFERENCES

Allen, M., Yung, Y. L., & Waters, J. W. 1981, J. Geophys. Res., 86, 3617
Chiar, J. E., Kutner, M. L., Verter, F., & Leous, J. 1994, ApJ, 431, 658
Clark, F. O., & Johnson, D. R. 1981, ApJ, 247, 104
Cohen, R. S., Dame, T. M., & Thaddeus, P. 1986, ApJS, 60, 695
Cowie, L. L., & McKee, C. F. 1977, ApJ, 211, 135
Dame, T. M. 1995, Calibration of the 1.2 m Telescopes, CfA Internal Rep. 4
Dame, T. M., Koper, E., Israel, F. P., & Thaddeus, P. 1993, ApJ, 418, 730
Dame, T. M., et al. 1987, ApJ, 322, 706
de Vries, H. W., Heithausen, A., & Thaddeus, P. 1987, ApJ, 319, 723
Dickey, J. M., & Garwood, R. W. 1989, ApJ, 341, 201
Elmegreen, B. G. 1993, in Protostars and Planets III, ed. E. H. Levy & J. I. Lunine (Tucson: Univ. Arizona Press), 97
Goerigk, W., Mebold, U., Reif, K., Kalberla, P. M. W., & Velden, L. 1983, A&A, 120, 63
Hartmann, D. 1994, Ph.D. thesis, Univ. Leiden
Heiles, C. 1990, in The Interstellar Disk-Halo Connection in Galaxies, ed. J. B. G. M. Bloemen (Dordrecht: Kluwer), 433
———. 1992, in Evolution of Interstellar Matter and Dynamics of Galaxies, ed. J. Paloŭs, W. B. Burton, & P. O. Lindblad (Cambridge: Cambridge Univ. Press), 12
Heiles, C., Reach, W. T., & Koo, B.-C. 1988, ApJ, 332, 313
Heithausen, A., Stacy, J. G., de Vries, H. W., Mebold, U., & Thaddeus, P. 1993, A&A, 268, 265
Heithausen, A., & Thaddeus, P. 1990, ApJ, 353, L49
Heyer, M. H., Carpenter, J. M., & Ladd, E. F. 1996, ApJ, 463, 630
Hilldith, R. W., Hill, G., & Barnes, J. V. 1976, MNRAS, 176, 175
Keto, E. R., & Myers, P. C. 1986, ApJ, 304, 466
Kilkenny, D. 1980, MNRAS, 191, 651
Knude, J. 1979, A&AS, 38, 407
Liszt, H. S. 1994, ApJ, 429, 638
Magnani, L., Blitz, L., & Mundy, L. 1985, ApJ, 295, 402 (MBM)
Magnani, L., Caillault, J.-P., Buchalter, A., & Beichman, C. 1995, ApJS, 95, 159
Magnani, L., Hartmann, D., & Speck, B. G. 1996, ApJS, 106, 447 (MHS)
Magnani, L., Lada, E. A., & Blitz, L. 1986, ApJ, 301, 395
Magnani, L., Onello, J. S., Adams, N., Hartmann, D., & Thaddeus, P. 1997, ApJ, submitted
Meyerdierks, H., Heithausen, A., & Reif, K. 1991, A&A, 245, 247
Norman, C. A. 1990, in The Interstellar Disk-Halo Connection in Galaxies, ed. J. B. G. M. Bloemen (Dordrecht: Kluwer), 337
Penprase, B. E. 1993, ApJS, 88, 433
Perry, C. L., & Johnston, L. 1982, ApJS, 50, 451
Polk, K. S., Knapp, G. R., Stark, A. A., & Wilson, R. W. 1988, ApJ, 332, 432
Reach, W. T., Koo, B.-C., & Heiles, C. 1994, ApJ, 429, 672
Scalo, J. M. 1985, in Protostars and Planets II, ed. D. C. Black & M. S. Matthews (Tucson: Univ. Arizona Press), 201
Snowden, S. L., McCammon, D., & Verter, F. 1993, ApJ, 409, L21
van Dishoeck, E. F., Black, J. H., Phillips, T. G., & Gredel, R. 1991, ApJ, 366, 141
Wannier, P. G., Andersson, B.-G., Federman, S. R., Lewis, B. M., Viala, Y. P., & Shaya, E. 1993, ApJ, 407, 163